

Temperature-time duality and deep level spectroscopies

Sandeep Agarwal

Department of Electrical Engineering, Indian Institute of Technology, Kanpur 208016, India

Y. N. Mohapatra and Vijay A. Singh

Department of Physics, Indian Institute of Technology, Kanpur 208016, India

(Received 20 October 1994; accepted for publication 12 December 1994)

Relaxation of deep levels in semiconductors is studied through capacitance transients. We explore the temperature-time duality relationship which is inherent in such thermal relaxation processes. Using duality considerations we show the existence of four distinct spectroscopies. We demonstrate that the techniques for spectroscopic evaluation of capacitance transients are based on differential operators and provide a novel interpretation to spectroscopy. We extend this approach to higher order spectroscopy. Two families of higher order spectroscopy are analyzed using the formalism of temperature-time duality and differential operators. From duality considerations we have suggested a novel deep level spectroscopy as well as various improvements in line shapes and spectroscopic quality of existing techniques. © 1995 American Institute of Physics.

I. INTRODUCTION

Relaxation studies of deep levels in semiconductors provide information relating to activation energy and capture cross section. After the early work of Sah *et al.*¹ and Lang,² capacitance transients have been widely utilized for deep level relaxation studies. Many spectroscopic variants of deep level transient spectroscopy (DLTS) have since been proposed.^{3–14} While there are many techniques for spectroscopic analysis of capacitance transients, they are treated as a loosely related family of spectroscopic tricks. In this article we have explored the temperature-time duality relationship which is inherent in the capacitance transient. We have also provided a novel interpretation of spectroscopy in which various spectroscopic methods are viewed as finite difference generalizations of differential operators. Using temperature-time duality considerations we show the deep interconnection that exists between various spectroscopic methods including higher order spectroscopy.^{15–17}

Early studies of deep levels were based on thermally stimulated current (TSC) and thermally stimulated capacitance (TSCAP) measurements.¹⁸ Single shot methods, however, were more accurate.¹ DLTS was introduced as an ingenious technique which retained the accuracy of single shot methods as well as the experimental ease of thermally stimulated methods.^{2–6} It is based on use of a rate window in *time* during a temperature scan. Another method termed paired temperature spectroscopy (PATS) involves a temporal scan with a window in *temperature*.^{7,8} There are many variants of the basic DLTS method to suit experimental requirements.^{9–12} There has also been an interest in isothermal spectroscopy for deep level analysis.^{13–15,19,20}

Temperature and time play a complementary role in the capacitance transient. Change of either temperature or time causes change in the transient signal. The complementary role of temperature and time extends to a wide range of phenomena in the physical sciences. For example, the probability that a particle can surmount an energy barrier is larger for smaller $\beta (=1/kT)$ or longer time. Similarly, the relationship between the quantum propagator and the classical par-

tition function is given by the transformation $t \rightarrow i\hbar/kT$ where \hbar is the Planck's constant and k the Boltzman's constant.²¹ We shall demonstrate that the underlying duality between time and temperature in the study of deep level phenomena is given as $\ln(t) \rightarrow -E/kT$ where E is the activation energy of the deep level. It will also be our endeavor in this article to demonstrate the utility of this formal view of temperature-time duality.

The article is organized as follows. In Sec. II the duality connection between temperature and time is explored using DLTS and PATS as concrete examples. In Sec. III we identify the differential operators associated with DLTS and PATS. In this section we also extend our analysis of temperature-time duality. Using duality considerations we derive two more spectroscopies: time analyzed transient spectroscopy (TATS), an isothermal spectroscopy defined in the time domain alone and temperature window transient spectroscopy (TWTS), defined in the temperature domain alone. Experimental realization for all four spectroscopies is presented. In Sec. IV we provide a general definition of higher order spectroscopy. We analyze two existing families of higher order spectroscopy and show that they are specific realizations arising from our general definition. We illustrate higher order TATS using data from the well-known DX center. Extension of higher order spectroscopy to PATS and TWTS is also discussed. Finally Sec. V carries a few practical suggestions arising out of duality considerations and a brief conclusion.

II. TEMPERATURE-TIME DUALITY

The capacitance transient exhibits characteristics that change both with temperature (T) and time (t). The junction capacitance is related to the trapped charge concentration. Experimentally a nonequilibrium occupation of traps is created and then relaxation of trapped charge is studied by monitoring capacitance transients. Its canonical form is given by

$$C(t, T) = C_0 \exp(-e_n t). \quad (1)$$

The emission rate, e_n , has an Arrhenius dependence on temperature

$$e_n = A T^2 \exp\left(\frac{-E}{kT}\right), \quad (2)$$

where E is the activation energy and A is related to the capture cross section of the trap. There is a large class of physical systems which have an activated relaxation mechanism.²² Experimental characterization is performed by use of an Arrhenius plot to obtain the relevant physical parameters from its slope and intercept.

A standard technique to obtain these points is DLTS. A complementary method, PATS, also gives identical information.^{7,8} In this section we outline a fruitful duality relationship between DLTS and PATS based on the temperature-time duality.

The capacitance transient for most practical purposes can be considered a simple exponential having a form given by Eq. (1). The DLTS signal is a function of temperature. It is constructed from the capacitance transient, $C(t, T)$, at a fixed rate window $\{t_1, t_2\}$

$$S(T) = C(t_1, T) - C(t_2, T). \quad (3)$$

The signal has a maximum at a temperature T_m . The emission rate at the maximum is given as

$$e_n = \frac{\ln(t_2/t_1)}{t_2 - t_1} \quad (4)$$

and peak value of the signal is proportional to $f(r)$ such that

$$f(r) = \left(\frac{1}{r}\right)^{\left(\frac{r}{r-1}\right)} (r-1), \quad (5a)$$

where

$$r = \frac{t_2}{t_1}. \quad (5b)$$

The PATS signal is a function of time, and can be constructed from the DLTS signal $S(T)$ by interchanging the role of time and temperature in Eq. (3). We thus obtain a signal which is derived from a fixed window in temperature $\{T_1, T_2\}$:

$$P(t) = C(t, T_1) - C(t, T_2). \quad (6)$$

$P(t)$ has a maximum in time t_m which is given as

$$t_m = \frac{\ln\left(\frac{\tau_1}{\tau_2}\right)}{\frac{1}{\tau_2} - \frac{1}{\tau_1}}, \quad (7)$$

where τ_1 and τ_2 are time constants (i.e., reciprocals of emission rates e_n) at temperatures T_1 and T_2 , respectively. The peak value of the PATS signal is proportional to $f(R)$ such that

$$f(R) = \left[\left(\frac{1}{R}\right)\right]^{[R/(R-1)]} (R-1), \quad (8a)$$

where

$$R = \frac{\tau_1}{\tau_2}. \quad (8b)$$

Equations (6) and (7) constitute paired temperature spectroscopy (PATS). An inspection of the DLTS and PATS expressions reveals an *appealing symmetry*. Time (t) in the DLTS expressions and the time constant (τ) in the PATS expressions are related by the transformation

$$t \rightarrow \frac{1}{\tau}. \quad (9)$$

Indeed using the above transformation, the PATS expressions (7) and (8) can be obtained from the DLTS expressions (4) and (5) and vice versa. Time constant (τ) is a function of temperature. Using the Arrhenius Eq. (2) and ignoring the weaker T^2 dependence in the pre-exponential, we obtain from expression (9)

$$\ln(t) \rightarrow -\frac{E}{kT}. \quad (10)$$

Expression (10) states the duality between time and temperature in thermal relaxation processes. The DLTS signal, which is a function of temperature, is related to the PATS signal, a function of time, by this transformation. The duality relationship also suggests that if the scale for viewing relaxation is $\ln(t)$ in the time domain then it is $(-1/T)$ in the temperature domain. The advantage of using these scales as spectroscopic axes is discussed in detail in Sec. V.

III. DUALITY AND THE DIFFERENTIAL LIMIT

In this section we first identify the differential operators associated with DLTS and PATS. We specifically show that both these spectroscopies are finite difference generalizations of differential operators. We then probe further into the notion of temperature-time duality. Using duality arguments we derive two additional spectroscopies. One of them, TATS is an isothermal spectroscopy while the other, TWTS is defined in the temperature domain alone.

A. Differential limit and spectroscopy

The spectroscopic character of the DLTS and PATS signals is not incidental. We first show that both DLTS and PATS expressions can be viewed as finite difference generalizations of differential operators. These differential operators are connected by temperature-time duality.

The capacitance transient in Eq. (1) can be expressed, using the duality expression (10), as

$$C(t, T) \rightarrow C[\ln(t), -1/T]. \quad (11)$$

The DLTS Eq. (3) can also be cast in a different fashion as

$$S[\ln(t), -1/T] = C[\ln(t), -1/T] - C[\ln(t) + \ln(r), -1/T], \quad (12)$$

where t_2/t_1 in Eq. (5a) has been replaced by r [Eq. (5b)]. When $r \rightarrow 1$, the differential limit of the DLTS signal is given by a simple Taylor expansion as

$$\lim_{\gamma \rightarrow 0} \frac{S[\ln(t), -1/T]}{\gamma} = - \frac{\partial C[\ln(t), -1/T]}{\partial \ln(t)} \quad (13a)$$

$$= \frac{t}{\tau} C[\ln(t), -1/T], \quad (13b)$$

where

$$\gamma = r - 1. \quad (13c)$$

The limit in Eq. (13a) shows that the DLTS signal is a finite difference generalization of the differential operator $\partial/\partial \ln(t)$. Differentiation of the capacitance transient [Eq. (1)] with respect to the logarithm of time (t) is equivalent to multiplication of the capacitance transient by (t/τ) and is given by Eq. (13b). This function has a maximum whose location and peak value have spectroscopic properties and is a generating function for the DLTS signal.

The PATS signal in Eq. (6) can also be cast in a different form in a similar fashion as

$$P[\ln(t), -1/T] = C[\ln(t), -1/T] - C[\ln(t), -1/T'], \quad (14a)$$

where

$$\frac{1}{T'} = \frac{1}{T} - \frac{1}{\Delta}. \quad (14b)$$

When $1/\Delta \rightarrow 0$, the PATS signal approaches its differential limit which is given as

$$\lim_{1/\Delta \rightarrow 0} \frac{P[\ln(t), -1/T]}{\frac{1}{\Delta}} = - \frac{\partial C[\ln(t), -1/T]}{\partial(-1/T)} \quad (15a)$$

$$= \frac{E}{k} \frac{t}{\tau} C[\ln(t), -1/T]. \quad (15b)$$

The PATS signal can also be viewed as a finite difference generalization of the differential operator $\partial/\partial(-1/T)$. Using Eq. (2) and ignoring the weaker T^2 dependence, we can replace $(-1/T)$ by the emission rate e_n such that

$$\frac{\partial C(t, T)}{\partial \ln(e_n)} \rightarrow \frac{k}{E} \frac{\partial C(t, T)}{\partial(-1/T)}. \quad (16)$$

Hence using Eq. (16) the differential limit of the PATS signal can also be expressed as $(E/k) \partial/\partial \ln(e_n)$. The DLTS differential operator $\partial/\partial \ln(t)$ and the PATS differential operator $\partial/\partial \ln(e_n)$ are related by the duality transformation $[\ln(t) \rightarrow -1/T]$ or alternatively $(t \rightarrow 1/\tau)$

$$\frac{\partial C[\ln(t), -1/T]}{\partial \ln(t)} \rightarrow \frac{\partial C[\ln(t), -1/T]}{\partial \ln(e_n)}. \quad (17)$$

The above correspondence is in fact an identity for any multiexponential signal. It implies that differentiation with respect to $\ln(e_n)$ is the spectroscopic dual of differentiation with respect to $\ln(t)$. The occurrence of trap energy in the differential operator for PATS [Eq. (15b)] leads to trap dependent features in the spectroscopy. This is further illustrated in Sec. V (Fig. 3).

B. Duality and novel spectroscopies

Capacitance transients can be viewed as surfaces in the three-dimensional space $\{C, t, T\}$. There is an information redundancy in the capacitance transient which makes it possible to design numerous methods for extraction of trap parameters. The transient changes both with time (t) and temperature (T). However it is not symmetric with respect to them. We first suggest a transformation of the variable space $\{t, T\}$ to $\{u, v\}$ such that the capacitance transient is symmetric in the new variable space

$$u = \ln(t),$$

$$v = \ln(e_n).$$

The capacitance transient in Eq. (1) can now be written as

$$C(u, v) = C_0 \exp[-\exp(u+v)]. \quad (18)$$

The capacitance transient is symmetric in the variable space $\{u, v\}$. Moreover, all its higher order partial derivatives are also symmetric. For example,

$$\frac{\partial C}{\partial u} = \frac{\partial C}{\partial v}, \quad (19)$$

$$\frac{\partial^2 C}{\partial u \partial u} = \frac{\partial^2 C}{\partial v \partial u} = \frac{\partial^2 C}{\partial u \partial v} = \frac{\partial^2 C}{\partial v \partial v}. \quad (20)$$

Note that the variable space $\{u, v\}$ is equivalent to $\{\ln(t), -1/T\}$. This suggests that the variable space $\{\ln(t), -1/T\}$ preserves the symmetry properties of the capacitance transient.

The first partial derivative of the capacitance transient has a distinct maximum when plotted against either (u) or (v). The location of the peak can be found by second partial differentiation. Equation (19) suggests four distinct and equivalent ways of finding the maximum, namely

$$\frac{\partial^2 C(u, v)}{\partial u \partial u} = 0 \quad (\text{TATS}), \quad (21)$$

$$\frac{\partial^2 C(u, v)}{\partial v \partial u} = 0 \quad (\text{DLTS}), \quad (22)$$

$$\frac{\partial^2 C(u, v)}{\partial u \partial v} = 0 \quad (\text{PATS}), \quad (23)$$

$$\frac{\partial^2 C(u, v)}{\partial v \partial v} = 0 \quad (\text{TWTS}). \quad (24)$$

All the above four equations have a solution:

$$v = -u,$$

or

$$e_n = \frac{1}{t}$$

and the peak value is given as C_0/e where e is the base of Napierian logarithm.

These four equivalent ways of finding the peak location correspond to four distinct spectroscopic techniques. The first expression is for a spectroscopy which is defined in the time domain alone and is termed TATS. It is an isothermal

spectroscopy. The last expression is for a novel spectroscopy termed TWTS. It is a thermally scanned technique with a window in temperature. This technique is defined over a constant time plane in the $\{C, t, T\}$ space. The TATS signal has a maximum at time t_m . The emission rate at this maximum is given by the DLTS Eq. (4) where $t_1 = t_m$. Similarly the peak value of the signal is given by the DLTS Eq. (5). The TWTS signal has a maximum at temperature T_m . The time constant τ at the maximum is related to time (t) by the PATS Eq. (7), where $t_m = t$ and $\tau_1 = \tau_m$. The peak value of the TWTS signal is given by the PATS Eq. (8).

With the exception of TATS, which is defined in the time domain alone [Eq. (21)], all the other three spectroscopies have trap-dependent features [Eqs. (22)–(24)]. This can be seen by noting that while the differential operator $\partial/\partial u$ is equivalent to $\partial/\partial \ln(t)$ in the real space, the differential operator $\partial/\partial v$ corresponds to $\partial/\partial(-E/kT)$. The dependence of the differential operator $\partial/\partial v$ on activation energy of the trap manifests itself in trap dependence of spectroscopy. (This is further discussed in Sec. V and illustrated in Fig. 3).

In Fig. 1 we show experimental realizations for the four spectroscopies defined above. The temperature axes have been plotted against the reciprocal of temperature ($1/T$) while time axes have been plotted as $\log(t)$. Transient signals were obtained for a gold related acceptor level in p -type silicon. Figure 1 illustrates the similarity of four techniques in terms of line shape and spectroscopic quality. This is to be expected from the symmetry of the capacitance transient in the $\{\ln(t), -1/T\}$ space.

IV. HIGHER ORDER SPECTROSCOPIES

In this section we extend the operator formalism to higher order spectroscopy. We begin by providing a general definition for spectroscopy applicable to higher order spectroscopy as well. We then analyze two existing families of higher spectroscopies and show that they are specific realizations of the above generalization. While higher order spectroscopy has been discussed in the literature in the context of DLTS we present our results for the case of TATS. We illustrate higher order spectroscopy with TATS using data from the well-known DX center. We also discuss extension of higher order spectroscopy to PATS and TWTS.

In the previous section we had demonstrated that first-order spectroscopy is a finite difference generalization of the first partial derivative. Higher order derivatives have multiple maxima/minima and they cannot be used for spectroscopic purposes directly. We generalize our definition of spectroscopy as follows:

$$S_n = \left(\frac{t}{\tau} \right)^n C(t, T), \quad (25)$$

where S_n denotes an n th order spectroscopy. S_n has a maximum in time (t) or temperature (T). The location of the maximum in time is given as

$$t_m = n\tau. \quad (26a)$$

and the peak value at the maximum is given as

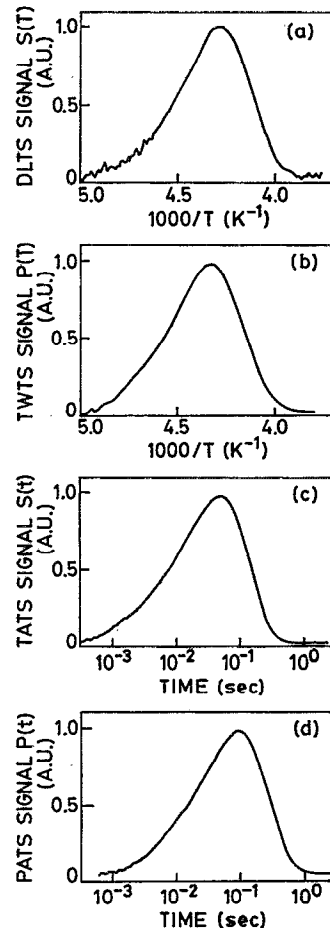


FIG. 1. Comparison of the four spectroscopic techniques. (a) DLTS, (b) TWTS, (c) TATS, (d) PATS. Data were acquired from commercial gold doped 2N2369 switching transistors. The dominant trap is a gold related acceptor level in p -type silicon having an activation energy $E=0.52$ eV. The DLTS curve has been processed for a value of $\tau=0.4$ s and $\gamma=1$. The TWTS curve is for $\Delta=5\times 10^4$ K. The TATS curve is at a temperature $T=245$ K for a value of $\gamma=1$. The PATS curve is acquired with $T_1=245$ K and $T_2=250$ K, $\Delta=1.225\times 10^4$ K for this choice of temperatures. The peak values of all four curves have been normalized for comparison. They have been plotted against the spectroscopic axes suggested by the duality expression (10).

$$S_n(t_m) = c_0 n^n \exp(-n), \quad (26b)$$

where n defines the order of spectroscopy. When $n > 1$ there are many possible finite differential generalizations of Eq. (25). Below we analyze two existing families of higher order spectroscopies and show that they are specific realizations of Eq. (25). Both families have earlier been conceptualized as tuned correlators. Our work suggests a deeper and more physical interpretation.

(i) *Arithmetic series*: This family of operators was originally suggested by Hodgart¹⁵ as an optimal correlation method to improve DLTS resolution. The original DLTS signal was constructed by taking data from values in time (t) which were in arithmetic progression. We obtain a corresponding TATS signal which is given as

$$S_n(t) = \binom{n}{0}(-1)^0 C(t, T_0) + \binom{n}{1}(-1)^1 C(t + \gamma t, T_0) + \dots + \binom{n}{n}(-1)^n C(t + n\gamma t, T_0), \quad (27)$$

where n is the order of spectroscopy. The signal $S_n(t)$ has a maximum in time t_m which is given as

$$t_m = \frac{\ln(1 + \gamma n)}{\gamma e_n}. \quad (28)$$

As the order of spectroscopy is increased, the linewidth reduces and consequently the resolution between two closely spaced peaks improves. The differential limit of the TATS signal $S_n(t)$ is given as

$$\lim_{\gamma \rightarrow 0} \frac{S_n(t)}{\gamma^n} = \left(\frac{t}{\tau}\right)^{n-1} \frac{\partial C(t, T)}{\partial \ln(t)} \quad (29a)$$

$$= \left(\frac{t}{\tau}\right)^n C(t, T). \quad (29b)$$

The differential limit of $S_n(t)$ is equivalent to Eq. (25). Hence the spectroscopy based on the above arithmetic series is a specific realization of higher order spectroscopy.

(ii) *Geometric Series:* This series was suggested by Crowell and Alipanahi¹⁶ and was further analyzed by Dmowski¹⁷ in the context of n th order correlation DLTS. We extend their coefficients to generate a TATS signal

$$S_n(t) = a_0 C(t, T_0) + a_1 C([1 + \gamma]t, T_0) + \dots + a_n C([1 + \gamma]^n t, T_0), \quad (30)$$

where the coefficients are given as

$$a_0 = 1, \quad a_1 = -1 \quad (n=1), \quad (31a)$$

$$a_0 = 1, \quad a_1 = -1 - \frac{1}{r}, \quad a_2 = \frac{1}{r} \quad (n=2), \quad (31b)$$

$$a_0 = 1, \quad a_1 = -1 - \frac{1}{r} - \left(\frac{1}{r}\right)^2, \\ a_2 = \frac{1}{r} + \left(\frac{1}{r}\right)^2 + \left(\frac{1}{r}\right)^3, \quad a_3 = -\left(\frac{1}{r}\right)^3 \quad (n=3). \quad (31c)$$

where $r = \gamma + 1$. In the limit $\gamma \rightarrow 0$ the geometric series approaches its differential limit such that

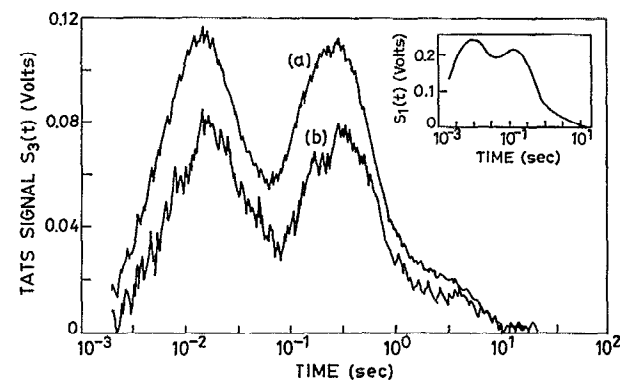


FIG. 2. Comparison of TATS curves for higher order spectroscopy. The transients have been acquired for silicon related DX center in $Al_{0.33}Ga_{0.67}As$ having a doping concentration of $4 \times 10^{17} \text{ cm}^{-3}$. The fill pulse duration used is 5 ms and the temperature $T = 185 \text{ K}$. (a) TATS based on $n=3$ geometric series and (b) TATS based on $n=3$ arithmetic series. The curves show multiple peaks corresponding to different states of the DX center. While TATS based on geometric series has better noise performance, it requires larger data storage. The inset shows $n=1$ first-order TATS for the same data. Note the significant improvement in peak resolution with higher order TATS.

$$\lim_{\gamma \rightarrow 0} \frac{S_1(t)}{\gamma} = - \frac{\partial C(t, T)}{\partial \ln(t)} \quad (32a)$$

$$= \left(\frac{t}{\tau}\right) C(t, T), \quad (32b)$$

$$\lim_{\gamma \rightarrow 0} \frac{S_2(t)}{\gamma^2} = \frac{\partial^2 C(t, T)}{\partial [\ln(t)]^2} - \frac{\partial C(t, T)}{\partial \ln(t)} \quad (32c)$$

$$= \left(\frac{t}{\tau}\right)^2 C(t, T). \quad (32d)$$

It can be seen from Eqs. (32b) and (32d) that the higher order spectroscopy based on the geometric series is also a specific realization of Eq. (25). However, while spectroscopies based on the arithmetic series are derived from the first partial derivative, those based on the geometric series are constructed from a linear combination of higher order partial derivatives.

Figure 2 shows experimental TATS curves for higher order spectroscopy with $n=3$ for the case of arithmetic and geometric series. The experimental data are from a silicon

TABLE I. The duality interrelationships of various spectroscopies. Symbols are identified in Secs. II and III B.

Spectroscopy	Differential operator	Spectroscopic axis	Window variable	Location of maxima	Peak value
DLTS	$\partial/\partial \ln(t)$	$-1/T$			
TATS		$\ln(t)$	$\ln\left(\frac{t_2}{t_1}\right)$	$\frac{1}{\tau_m} = \frac{\ln(t_2/t_1)}{t_2 - t_1}$	$\left(\frac{1}{r}\right)^{\frac{r}{r-1}} (r-1)$ $r = t_2/t_1$
TWTS	$\partial/\partial \ln(-1/T)$	$-1/T$	$\frac{1}{T_1} - \frac{1}{T_2}$	$t_m = \frac{\ln(T_1/T_2)}{(1/T_2) - (1/T_1)}$	$\left(\frac{1}{R}\right)^{\frac{R}{R-1}} (R-1)$
PATS		$\ln(t)$			$R = \tau_1/\tau_2$

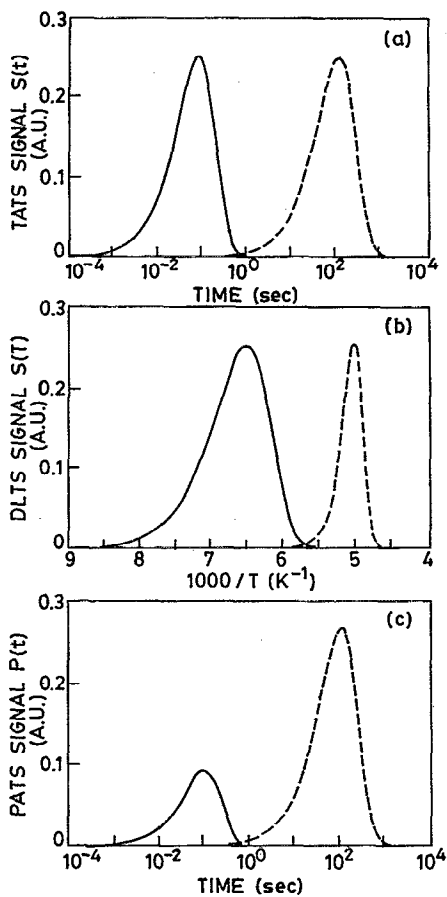


FIG. 3. Change in line shape and peak value of TATS, DLTS, and PATS signals with a change in trap parameters. (a) TATS signal, (b) DLTS signal, (c) PATS signal. Dashed line is for trap 1 while solid line is for trap 2. Trap 1 has $E=0.2$ eV, $A=1\times 10^7$ s⁻¹ K⁻². Trap 2 has $E=0.6$ eV, $A=2\times 10^8$ s⁻¹ K⁻². Both traps have the same concentration. TATS signal is plotted at $T=100$ K for trap 1 and at $T=200$ K for trap 2. The value of $\gamma=1$ [Eq. (13)]. DLTS signal is plotted for a rate window {10, 20 μ s} for trap 1 and {100, 200 s} for trap 2. PATS signal is plotted at a temperature $T=100$ K for trap 1 and $T=200$ K for trap 2. Temperature windows are for $\Delta=1\times 10^4$ K [Eq. (14b)]. Note that the TATS signal has identical line shape and peak value for the two traps. For the DLTS curves the peak value remains the same but the line shape changes. In the case of PATS both the line shape and the peak values are different for a choice of two different trap parameters.

related DX center in Al_{0.33}Ga_{0.67}As. The signal has three peaks. It can be seen that the geometric series leads to a better signal to noise ratio in comparison to the arithmetic series. However this is at a cost of longer data sequence which is required for the geometric series.

While the higher order spectroscopy has been analyzed using the TATS signal, a similar extension can be made to the case of PATS and TWTS. The TWTS signal can be written as

$$\begin{aligned} P_n(-1/T) = & a_0 C(t, -1/T) + a_1 C(t, -1/T + 1/\Delta) \\ & + a_2 C(t, -1/T + 2/\Delta) \\ & + \dots + a_n C(t, -1/T + n/\Delta). \end{aligned} \quad (33)$$

In the limit $1/\Delta \rightarrow 0$ the TWTS signal $P_n(-1/T)$ can be represented as a linear combination of higher order partial

derivatives. Since differentiation with respect to temperature ($-1/T$) makes the coefficient for higher order spectroscopy dependent on the activation energy of the trap [Eq. (15b)] a general trap-independent solution for the coefficients in Eq. (33) becomes difficult.

Search for optimization regarding resolution and signal to noise ratio in DLTS signal processing of transients has in the past led to several suggestions of higher order spectroscopy as specific realizations of tuned correlators. This was being pursued vigorously until recently, taking full advantage of digital signal processing. However in this section we have demonstrated a theoretical basis of higher order spectroscopy, providing a unifying theme and physical insights.

V. DISCUSSION AND CONCLUSIONS

There is an information redundancy in the capacitance transient which makes it possible to design numerous methods for extraction of trap parameters. We can classify the temperature-time combinations used by experimental methods in deep level studies as follows: (1) scanning of temperature at a fixed time, (2) scanning of time at a fixed temperature, and (3) scanning of temperature linearly with time. These cases correspond to a constant time plane, a constant temperature plane, or a diagonal plane in the three dimensional $\{C, t, T\}$ space. The DLTS technique explores two planes of constant times t_1 and t_2 . PATS is based on two planes of constant temperatures T_1 and T_2 . TATS is a time domain technique defined over a constant temperature plane. We have also proposed a fourth spectroscopy, TWTS, which is based on a constant time plane. Using temperature time duality we have shown the interconnection between the four different spectroscopies. We have also shown that all four deep level spectroscopies are finite difference generalizations of differential operators.

Higher order spectroscopy is based on a product of the function $(t/\tau)^n$ with the capacitance transient. There are many possible ways of realizing higher order spectroscopy. While we have analyzed the case of TATS, extensions can be made to the remaining three spectroscopies. Similarly, although the article discusses the case of a simple exponential transient, the analysis can be extended to the case of multi-exponential and nonexponential transients.

Temperature-time duality manifests itself at many levels in deep level spectroscopy: (i) in the choice of spectroscopic axes, (ii) in the choice of differential operator, and (iii) in the symmetry of expressions involving peak positions and peak values. Table I contains a brief summary of the temperature-time duality in the context of deep level relaxation.

All four transient spectroscopies are inter-related. However they differ in their information content and spectroscopic character. In Sec. II it was suggested that the relevant scale of spectroscopic axes for temperature is $1/T$ and for time it is $\ln(t)$. It can be shown that the DLTS and TWTS line shapes shed their dependence on rate window if plotted as a function of $(1/T)$ instead of temperature (T). Similarly the TATS and PATS line shapes become more symmetric when plotted as a function of $\ln(t)$ instead of time (t).

Our analysis of spectroscopic operators shows that spectroscopies involving temperature as a scanning variable would involve trap parameters in their corresponding operators. We demonstrate such dependence by comparing line shapes and peak values of DLTS, PATS, and TATS for a choice of two different trap parameters. Figure 3 shows a comparison of the line shapes and peak values of the DLTS, PATS, and TATS for a choice of two different trap parameters. It can be seen that the TATS line shape and peak value do not depend upon the trap parameters. For DLTS only the peak value is independent of trap activation energy and capture cross section. However for the case of PATS, both the line shape and peak value depends upon the trap activation energy and capture cross section.

In many cases of deep level analysis, scanning in temperature introduces nonexponentiality due to temperature-dependent change in the strength of the capacitance transient. This is known to occur in the case of the DX centers in III-V compounds,^{23,24} Pt in silicon,²⁵ Ag and Au in GaAs.²⁶ In such cases, analysis of capacitance transients can become quite involved and intractable for DLTS, TWTS, and PATS analysis. TATS being an isothermal spectroscopy overcomes these inherent difficulties. Moreover, being a time domain technique, it can be also used in the analysis of *athermal* relaxation processes such as photoionization current or capacitance transients, photoconductivity decay transients, etc.

ACKNOWLEDGMENTS

We would like to thank Dr. R. Sharan, Dr. B. M. Arora, and Dr. B. Mazhari for fruitful discussions. One of us (V.A.S.) acknowledges support provided by the Department of Science and Technology, Govt. of India (Grant No. SP/S2/M-39/87).

- ¹C. T. Sah, L. Forbes, L. L. Rosier, and A. F. Tasch, Solid-State Electron. **13**, 759 (1970).
- ²D. V. Lang, J. Appl. Phys. **45**, 3023 (1974).
- ³D. V. Lang, *Thermally Stimulated Relaxation in Solids*, Topics in Applied Physics Vol. 37, edited by P. Braunlich (Springer, Berlin, 1979), pp. 93–133.
- ⁴G. L. Miller, D. V. Lang, and L. C. Kimmerling, Annu. Rev. Mater. Sci. **7**, 377 (1977).
- ⁵G. L. Miller, J. V. Ramirez, and D. A. H. Robinson, J. Appl. Phys. **46**, 2638 (1975).
- ⁶P. J. Dean, A. G. Cullis, and A. M. White, *Handbook of Semiconductors*, edited by Seymour P. Keller (North Holland, Amsterdam, 1980), Vol. 3, pp 113–215.
- ⁷Raj K. Singh, Vijay A. Singh, J. W. Corbett, and A. Das, J. Phys. C, Solid State Phys. **19**, 2177 (1986).
- ⁸Raj K. Singh, Vijay A. Singh, and J. W. Corbett, Semicond. Sci. Technol. **2**, 716 (1987).
- ⁹N. M. Johnson, D. J. Bartelink, R. B. Gold, and J. F. Gibbons, J. Appl. Phys. **50**, 4828 (1979).
- ¹⁰A. Chantre, G. Vincent, and D. Bois, Phys. Rev. B **23**, 5355 (1981).
- ¹¹C. Hurtes, M. Boulou, A. Mitonneau, and D. Bois, Appl. Phys. Lett. **32**, 821 (1978).
- ¹²J. W. Farmer, C. D. Lamp, and J. M. Meese, Appl. Phys. Lett. **41**, 1063 (1987).
- ¹³Hideyo Okushi and Yozo Tokumaru, Jpn. J. Appl. Phys. **19**, L335 (1980).
- ¹⁴P. M. Henry, J. M. Meese, J. W. Farmer, and C. D. Lamp, J. Appl. Phys. **57**, 628 (1985).
- ¹⁵M. S. Hodgart, Electron Lett. **14**, 388 (1978); **15**, 724 (1979).
- ¹⁶C. R. Crowell and S. Alipanahi, Solid-State Electron. **24**, 25 (1980).
- ¹⁷K. Dmowski, Rev. Sci. Instrum. **61**, 1319 (1990).
- ¹⁸M. C. Driver and G. T. Wright, Proc. Phys. Soc. (London) **81**, 141 (1963); J. C. Carballés and J. Lebailly, Solid State Commun. **6**, 167 (1968).
- ¹⁹L. R. Tessler, F. Alvarez, and O. Teschke, Appl. Phys. Lett. **62**, 2381 (1993).
- ²⁰L. Dobaczewski, P. Kaczor, M. Missous, A. R. Peaker, and Z. R. Zytkiewicz, Phys. Rev. Lett. **68**, 2508 (1992).
- ²¹H. Feshback, Physics Today, p. 9, Nov. (1987); C. Kittel, *ibid.* p. 93, May (1988).
- ²²S. L. Miller, P. J. McWhorter, W. M. Miller, and P. V. Dressendorfer, J. Appl. Phys. **70**, 4555 (1991).
- ²³Z. Su and J. W. Farmer, Appl. Phys. Lett. **59**, 1746 (1991).
- ²⁴J. C. Bourgoin, S. L. Feng, and H. J. von Bardeleben, Phys. Rev. B **40**, 7663 (1989).
- ²⁵S. D. Brotherton, M. J. King, and G. J. Parker, J. Appl. Phys. **52**, 4649 (1981).
- ²⁶Z. X. Yan and A. G. Milnes, J. Electrochem. Soc. **129**, 1353 (1982).